Comparison of different numerical modelling techniques to evaluate high-speed crushing behaviour of fibre-reinforced composites

Christian Pohl[1], Huifang Liu[2], Drew E. Sommer[2], Daniel Thomson[2], Justus Hofmann[2], Nik Petrinic[2]

[1] Technical University of Munich, TUM Department of Aerospace and Geodesy, Chair of Carbon Composites, Germany

[2] Department of Engineering Science, University of Oxford, Oxford

18th European Mechanics of Materials Conference, April 4th-6th, 2022, Oxford

Agenda

1 Motivation
2 Experimental approach
3 Numerical representation
4 Evaluation of numerical predictions
5 Conclusions and outlook

Motivation

- Elevated strain rates change the mechanical response of fibre-reinforced composites

- The loading rate dependency of material properties plays a role in axial crushing

- Crushing has so far mainly been evaluated on component-level structures

→ **Coupon crushing experiments and accompanying simulation campaign to improve understanding of failure behaviour in composites!**

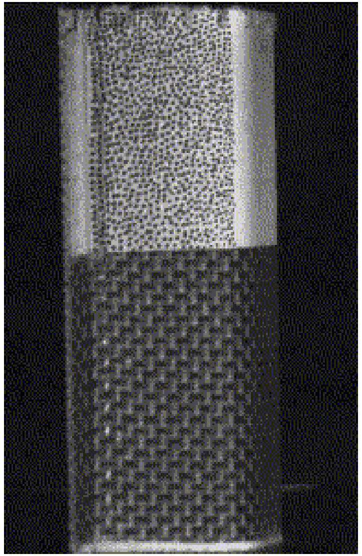

Fig. 1: Dynamic crushing test of a carbon/aramid-epoxy laminate omega profile [1]

Experimental approach – Specimens

- A Through-Thickness Trigger (TTT) specimen geometry proposed by Bru et al. was adapted [2]

- A trigger angle of 20° and a free length of 10 mm showed the most promising results in preliminary studies

- Manufactured from carbon-epoxy material IM7/8552 with a 2 mm thick quasi-isotropic laminate ($[90°/0°/\pm45°]_{2s}$)

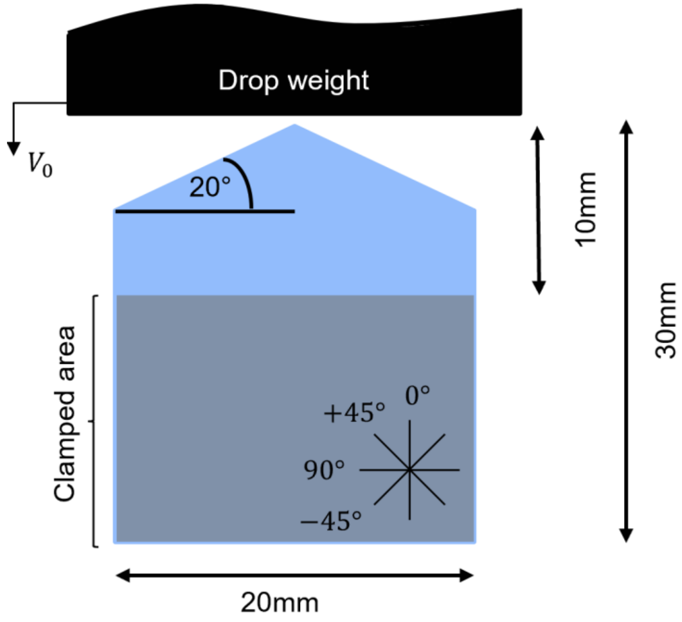

Fig. 2: Dimensions and mounting of adapted TTT specimen

Experimental approach – Test setup

- Tests on drop-tower setup with 15.3 kg impactor at 1.5 m/s impact velocity

- 2 high-speed cameras at 120,000 fps

- Analysis of obtained images via Digital-Image-Correlation

- The force was computed by differentiating the measured displacement twice and multiplying by the drop weight mass

- Smoothing of signals with 3 kHz sliding mean filter

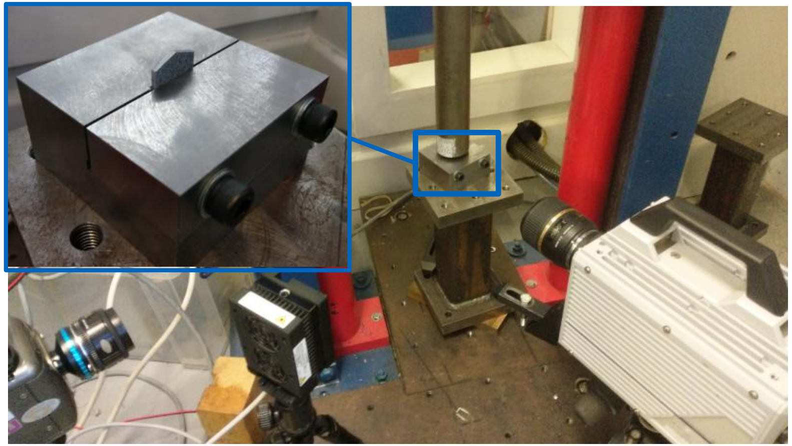

Fig. 3: Measures of adapted TTT specimen

Numerical representation – Input data

- IM7/8552 has been thoroughly studied under quasi-static and dynamic loads

- All inter- and intralaminar elastic properties, strengths and fracture toughnesses were characterized in previous studies

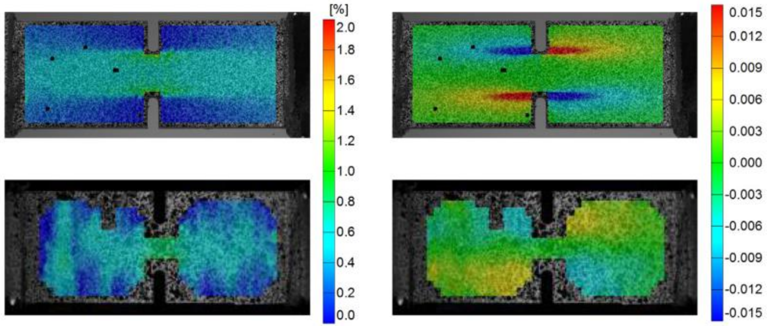

Fig. 4: Double-Edge-Notched-Tension specimens‘ axial (left) and shear strain fields under quasi-static (top) and high-rate loading conditions [3]

Numerical representation – Intralaminar model

- LS-DYNA selected as solver in underlying project

- *MAT_ENHANCED_COMPOSITE_ DAMAGE (*MAT_058) is used due to stable performance

- Included intralaminar fracture toughnesses to represent damage evolution

- Quasi-static (QS) and fully strain-rate-dependent (HR) material definition applied in separate models

- Implemented strain rate increase factor of:

$$f(\dot{\varepsilon}) = 1 + (K \cdot \dot{\varepsilon})^{\frac{1}{n}} \quad [4]$$

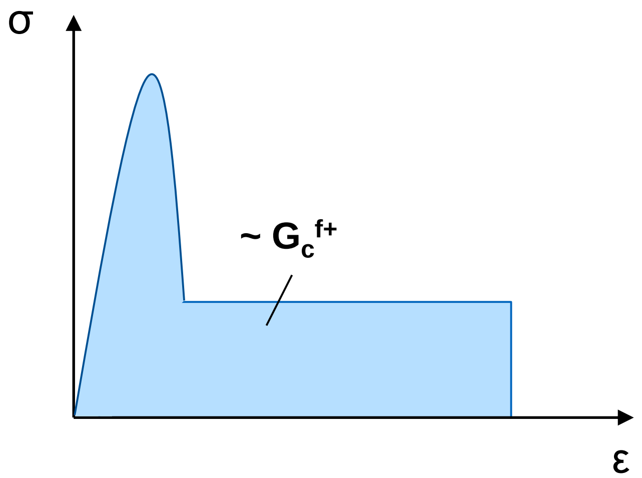

Fig. 5: Schematical stress-strain behavior of *MAT_058 in fiber tensile direction

Numerical representation – Interlaminar model

- *MAT_COHESIVE_MIXED_MODE_ELASTO-PLASTIC_RATE (*MAT_240) or equivalent TIEBREAK model (Option 14) is used to represent delamination failure

- Experimental data from literature were used for mode I and II crack opening calibration [5,6]

- Quasi-static (QS) and fully strain-rate-dependent (HR) material definition applied in separate models

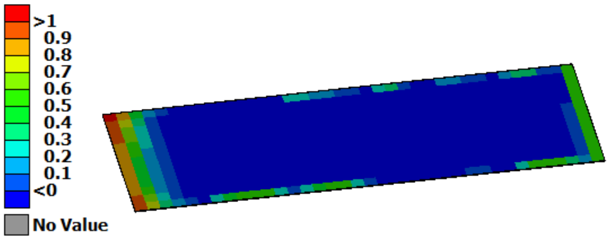

Fig. 6: DCB deformation behavior and damage variable of *TIEBREAK-contact

Numerical representation – FE model

- Ply-by-ply model (16S) with cohesive interfaces or stacked sub-laminate model (4S) with TIEBREAK interfaces

- Aligned mesh in trigger zone to mitigate numerical noise

- Exploiting symmetry, fixture modelled as rigid

- Initial velocity and gravitational force applied to rigid drop weight, friction coefficient 0.3

- Same filter frequency as in experiments applied

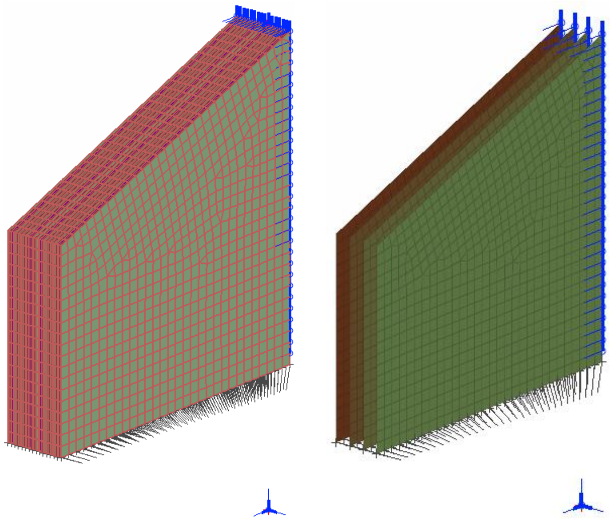

Fig. 7: Comparison of 16S model (left) with 4S model (right)

Evaluation of numerical predictions – Force-disp. curves

Δ < 2*STDV		Max. Force (N)	Mean Force (N)	Max. Disp. (mm)
EXP	**Value**	6291	2950	6.57
	STDV	639	395	0.92
	CV	10.2%	13.4%	14.0%
SIM	**16S_HR**	3633	**2204**	8.57
	16S_QS	2233	1462	9.63
	4S_HR	**7532**	**3629**	**5.05**
	4S_QS	**5069**	**2161**	8.74

Tab. 1: Force and displacement statistics of TTT experiments and simulations

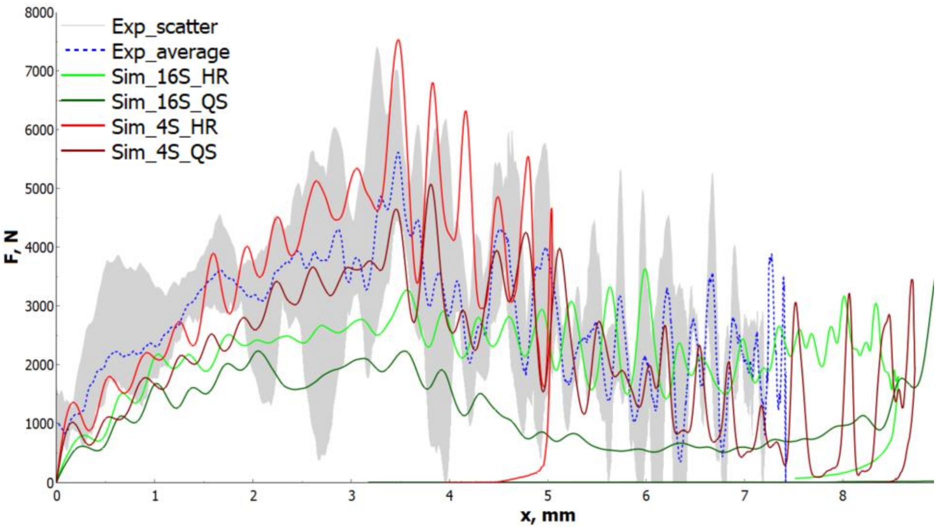

Fig. 8: Force-displacement-diagram of TTT experiments and simulations

Evaluation of numerical predictions – Damage behaviour

- Experiments exhibit a combination of splaying in outer layers and fragmentation in inner layers

- Observed behaviour is in line with descriptions from literature [2]

- In simulations, the 4S response is too stiff, whereas 16S exaggerates the deformation

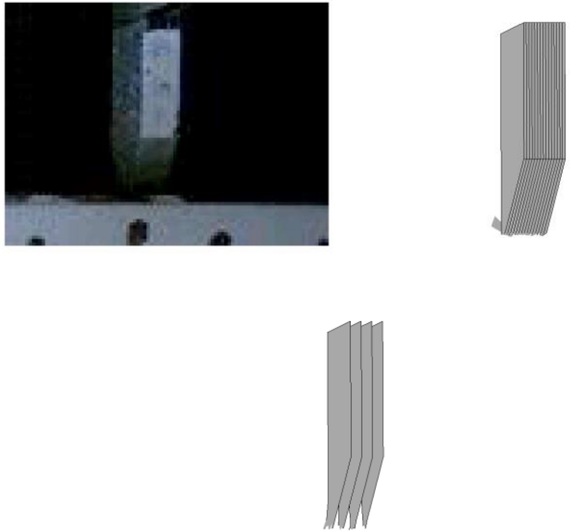

Fig. 9: Lateral view on specimen crushing in experiment, 16S_HR (right) and 4S_HR simulation (lower picture)

Evaluation of numerical predictions – Strain rates

- Both, experiments and simulations indicate the existence of local strain rates 10 to 15 times above the nominal strain rate

- Justifies the application of numerically more costly strain-rate-dependent material definitions

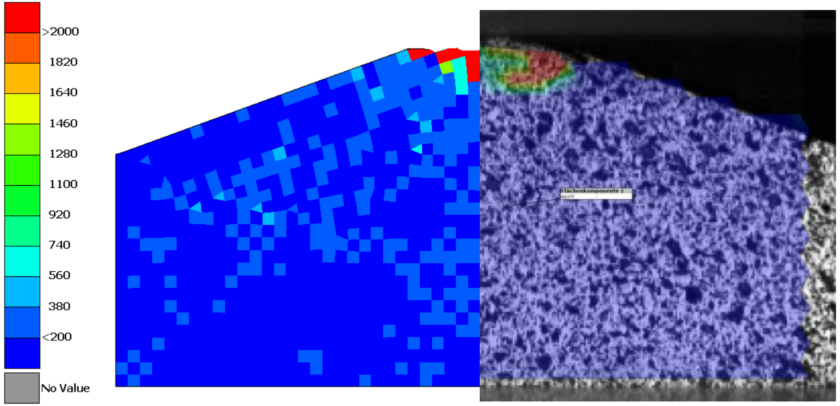

Fig. 10: Comparison of strain rate field in loading direction at t = 0.4 ms for 4S_HR (left) simulation and experiment (right)

Conclusions and outlook

- Strain-rate-dependent material representation is necessary in highly dynamic composite applications
- 4S models provide very runtime-efficient predictions close to experimental results
- Further experiments with higher impact velocities on split-Hopkinson-Bars
- Comparison with solid element ply-by-ply models
- Further assessment of delamination using improved calibration of models

	Runtime (s)	Elements
16S_HR	19883	23717
4S_HR	938	3209

Tab. 2: Simulation runtime comparison (28 CPU Intel Xeon E5-2690 v3, LS-DYNA R11.1 MPP)

Thank you for your attention!

Questions?

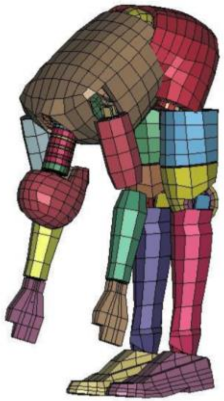

[7]

References

[1] Pieper T. Erweiterung und Validierung von Faserverbund-Materialkarten zur simulativen Beschreibung des Crushingverhaltens. Semester Thesis. Technical University of Munich; 2021.

[2] Bru T, Waldenström P, Gutkin R, Olsson R, Gaurav MV. Development of a test method for evaluating the crushing behavior of unidirectional laminates. Journal of Composite Materials 2017;Vol. 51 (29) 4041–4051.

[3] Kuhn P, Catalanotti G, Xavier J, Ploeckl M, Koerber H. Determination of the crack resistance curve for intralaminar fiber tensile failure mode in polymer composites under high rate loading. Composite Structures 2018;204:276–87.

[4] Koerber H. Mechanical response of advanced composites under high strain rates. PhD Thesis; Porto; University of Porto; 2010.

[5] Czabaj MW, Ratcliffe JG. Comparison of intra and interlaminar mode-I fracture toughness of unidirectional IM7/8552 graphite/epoxy composite. Composites Science and Technology 2013;89:15-23.

[6] O'Brien KT, Johnston WM, Toland GJ. Mode II interlaminar fracture toughness and fatigue characterization of a graphite epoxy composite material. 2010.

[7] Dynamore Webinar Composite-Berechnung, https://www.dynamore.de/de/download/presentation/dokumente/copy_of_download-Envyo%20und%20Composite-Berechnung/copy5_of_02_DYNAmore_Webinar_Optimierung_mit_LS-OPT_03_2017, 2017